

LETTER TO THE EDITOR

Observation of ion temperatures exceeding background electron temperatures in petawatt laser-solid experiments

P A Norreys^{1,9}, K L Lancaster^{1,2,9}, H Habara^{1,9,10}, J R Davies³,
J T Mendonça^{1,3}, R J Clarke¹, B Dromey⁴, A Gopal², S Karsch^{1,11},
R Kodama^{5,10}, K Krushelnick², S D Moustazis⁶, C Stoeckl⁷,
M Tatarakis⁸, M Tampo⁵, N Vakakis⁶, M S Wei² and M Zepf⁴

¹ Rutherford Appleton Laboratory, Chilton, Didcot, Oxon OX11 0QX, UK

² Blackett Laboratory, Imperial College of Science, Technology & Medicine, Prince Consort Road, London SW7 2BZ, UK

³ GoLP, Instituto Superior Tecnico, 1049-001 Lisboa, Portugal

⁴ Department of Pure and Applied Physics, Queens University of Belfast, Belfast BT7 1NN, UK

⁵ Institute of Laser Engineering, Osaka University, Osaka 565, Japan

⁶ Institute of Matter Structure and Laser Physics, Technical University of Crete, 73100 Chania, Crete, Greece

⁷ Laboratory of Laser Energetics, University of Rochester, 251 East River Road, Rochester NY, USA

⁸ Technological Educational Institute of Crete, Laboratory of Optoelectronics, Lasers and Plasma Technology, 73133 Chania, Crete, Greece

Received 18 July 2005, in final form 19 August 2005

Published 5 October 2005

Online at stacks.iop.org/PPCF/47/L49

Abstract

Neutron time of flight signals have been observed with a high resolution neutron spectrometer using the petawatt arm of the Vulcan laser facility at Rutherford Appleton Laboratory from plastic sandwich targets containing a deuterated layer. The neutron spectra have two elements: a high-energy component generated by beam-fusion reactions and a thermal component around 2.45 MeV. The ion temperatures calculated from the neutron signal width clearly demonstrate a dependence on the front layer thickness and are significantly higher than electron temperatures measured under similar conditions. The ion heating process is intensity dependent and is not observed with laser intensities on target below $10^{20} \text{ W cm}^{-2}$. The measurements are consistent with an ion instability driven by electron perturbations.

Electron and ion energy transport in dense plasmas is an extremely important topic in fast ignitor research for inertial fusion energy [1]. Recent experiments indicate that the hot electrons

⁹ These authors contributed equally to this work.

¹⁰ Present address: Graduate School of Engineering, Osaka University, Japan.

¹¹ Present address: Max Planck Institute for Quantum Optics, Garching, Germany.

generated at the plasma surface carry about 50% of the laser energy into the over-dense plasma. However, the fast electron current propagation involves very complex processes that arise from the strong electric and magnetic fields which are induced and significantly affect its propagation.

Recent experiments have measured the background electron temperature of the bulk material by resonance line emission from buried Al signature layers inside solid plastic targets [2, 3]. It is interesting to note that the background electron temperature measured there may have been affected by resistivity mismatching between the plastic and metal layers [4]. Taking this effect into account in hybrid code computer simulations, the measurements indicated that there was an energy barrier on the front surface of the target that reduced the fast electron energy transport into the bulk of the target, resulting in smaller background electron heating [3].

We report here the first observations of the ion temperature gradient in solid density plasmas using a single PW-class laser beam that cast new light on this anomalous resistivity effect. The laser pulse was incident onto plastic ‘sandwich’ targets that contain a signature layer of deuterated plastic. It is demonstrated from the derived neutron spectra that the ion temperatures in the surface layers are very much larger than the measured electron temperatures under similar irradiation conditions. There is a clear intensity dependence on the ion heating process. These observations are consistent with a plasma instability model that cascades the laser energy directly towards the ion population without significant background electron heating.

The experiment was conducted using the PW laser facility at Rutherford Appleton Laboratory [5]. The PW laser pulse irradiated 140 μm -thick plane deuterated plastic (CD_2) targets as well as sandwich targets that consisted of a variable thickness front plastic (CH_2) layer, a fixed 168 (± 5) μm CD_2 thickness layer, followed by a rear plastic layer (CH_2) of 195 (± 5) μm . The targets were designed to remove any boundary layer heating processes due to density and Z mismatches and were sufficiently thick to minimize heating due to refluxing electrons from the rear surface. The laser pulse was incident at an angle of 45° from the target normal. Up to 400 J was incident onto target in 1 ps pulse duration, corresponding to a peak focused intensity of $4 \times 10^{20} \text{ W cm}^{-2}$ with 40% of the laser energy within a 7 μm diameter focal spot.

The laser pulse intensity contrast ratio was $\sim 5 \times 10^{-8}$. This pre-pulse is associated with amplified spontaneous emission and has a duration equal to half of that of the stretched pulse in the amplifier chain, which is 3 ns in duration. Two-dimensional hydrodynamic simulations indicated that this pre-pulse generates a plasma with a density scale-length of 3 μm . The scale-length was found to be insensitive to contrast ratios between 10^{-6} and 10^{-8} for these focal spot dimensions, indicating that lateral transport of energy occurs as the intensity of the pre-pulse rises. Another indication that the contrast ratio was high during these experiments came from shots using a 1 μm -thick deuterated plastic foil from which x-ray and neutron yields similar to those from thick target were measured. A large pedestal or pre-pulse would have exploded the foil before the interaction pulse arrived.

The neutron signals were observed using the multi-channel neutron detector system, LaNSA [6, 7], that has been reconstructed in the Vulcan PW target area. The 1.6 m \times 1.6 m detector array comprises 256 Thorn-EMI 9902KB05 photo-multiplier tubes that were coupled to Bicorn 505 liquid scintillators. The signal from each knock-on proton scintillation event was fed into CAMAC and fastbus modules that were controlled through an IBM compatible personal computer. The signals were delivered to a LeCroy 1879 time-to-digital converter that recorded the arrival time of each event via a LeCroy 4413 discriminator. These arrival times were recorded and converted into a neutron spectrum via the time of flight method.

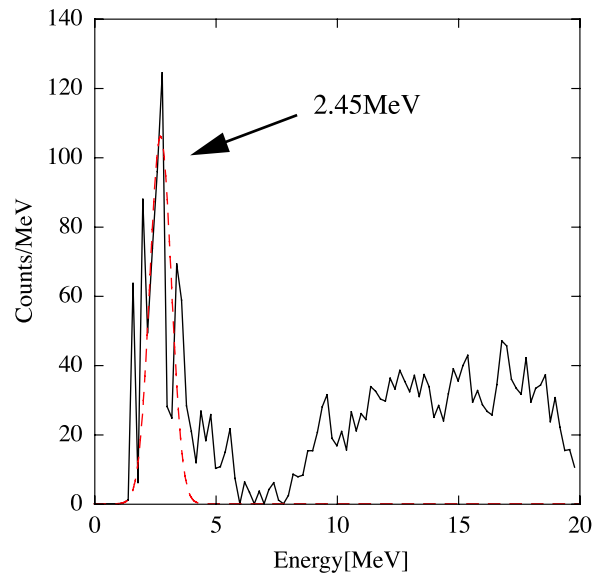


Figure 1. Neutron signal from the LaNSA instrument with a $140\ \mu\text{m}$ -thick CD_2 target irradiated with $286\ \text{J}$ ($3 \times 10^{20}\ \text{W cm}^{-2}$) on target. In converting to dN/dE , the bin size was chosen to be the energy resolution of the instrument ($45\ \text{keV}$). Also shown is the Gaussian fit to this spectrum (- - -). The chi-squared of the fit is 12 000 and the R -value is 0.86. The error resulting from the fitting procedure is 6.9%. However, when the energy resolution of neutron spectrum is changed from a minimum energy resolution of $33\ \text{keV}$ to a much larger resolution of $200\ \text{keV}$, the energy width from the Gaussian fitting is strongly affected. The changes, $\sqrt{(\text{energy width}^2 - \text{resolution}^2)}$, are 39%. This larger value was taken for the measurement error.

(This figure is in colour only in the electronic version)

The distance from the chamber centre was $12.9\ \text{m}$, giving an energy resolution of $45\ \text{keV}$ for $2.45\ \text{MeV}$ neutrons. The target was orientated so that the LaNSA detector was 18° from the front surface target normal. A systematic centring error associated with leading edge event timing of the x-ray signal fiducial was calculated to be $\pm 0.32\ \text{MeV}$. The dynamic range of the instrument in its current configuration in the Vulcan PW target area was two orders of magnitude.

Collimation to the target chamber centre was provided by $60\ \text{cm}$ -thick boron impregnated concrete blocks. They shielded the instrument from scattered photons and particles and were augmented by $22\ \text{cm}$ of lead shielding that reduced the x-ray flash associated with the PW laser pulse interaction to a level that allowed the photomultiplier tubes sufficient time to recover before the neutron arrival time.

Figures 1–3 show typical neutron spectra. The spectra showed distinct peaks at $2.45 \pm 0.32\ \text{MeV}$, the error coming from the systematic uncertainty in the time-of-flight, and a series of smaller peaks at higher energies, which varied from shot-to-shot. The width and height of the peak at $2.45\ \text{MeV}$ decreased with increasing front CH_2 thickness. When a $139\ \mu\text{m}$ -thick CD_2 target was irradiated with $68\ \text{J}$ on target corresponding to an intensity on target of $7 \times 10^{19}\ \text{W cm}^{-2}$, closer to the intensities used in previous experiments, no neutron signal was observed in the detector at $2.45\ \text{MeV}$, as shown in figure 4. It therefore appears that there is a distinct intensity threshold for this phenomenon.

Neutron emission has been observed in previous experiments with deuterated targets and were attributed to beam-fusion reactions [8]. Beam-fusion is associated with a shift in the

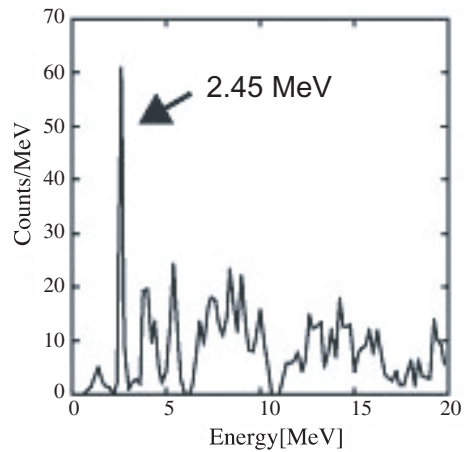


Figure 2. Neutron signal from a $3\ \mu\text{m CH}_2/168\ \mu\text{m CD}_2/195\ \mu\text{m CH}_2$ sandwich target irradiated by $428\ \text{J}$ ($4 \times 10^{20}\ \text{W cm}^{-2}$) on target. Notice that the neutron peak at $2.45\ \text{MeV}$ is much narrower and the number of counts/MeV is reduced.

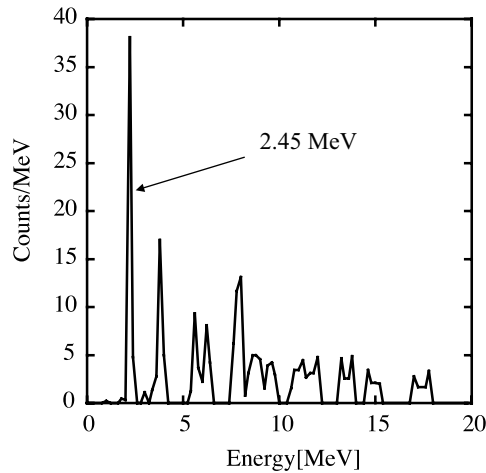


Figure 3. Neutron signal from a $10\ \mu\text{m CH}_2/168\ \mu\text{m CD}_2/195\ \mu\text{m CH}_2$ sandwich target irradiated by $400\ \text{J}$ ($4 \times 10^{20}\ \text{W cm}^{-2}$) on target. The chi-squared for this data point is 0.24 and R -value is 0.99991 . Although the error from fitting is 2.2% , the width increases to 200.4% at $200\ \text{keV}$ resolution, due to the small number of counts.

neutron peak caused by the centre-of-mass velocity of the beam, which is measured to be $0 \pm 0.32\ \text{MeV}$. The width and shape of the peak are associated with the spread in velocities of the deuterons, which, within the resolution of the measurements, are symmetric and well fitted by a Gaussian. We therefore fitted the peaks at $2.45\ \text{MeV}$ using results obtained for thermonuclear fusion to obtain a deuteron temperature. In other words, we assumed that the deuteron distribution in the layer was given by a three-dimensional Maxwellian. Nevertheless, it must be stressed that all that can be determined with any certainty from these measurements is the variance of the deuteron velocity within the deuterated layer in the direction of the target normal. The interested reader is referred to the paper by Slaughter [9] who discusses non-Maxwellian, beam-fusion neutron distributions in some detail.

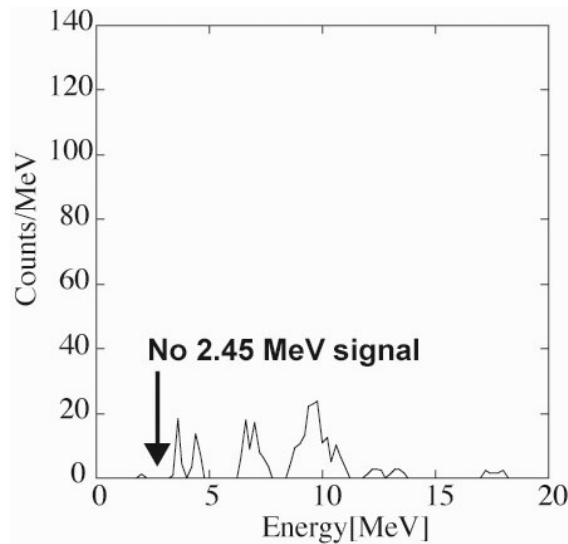


Figure 4. Neutron signal from a $140\ \mu\text{m}$ -thick CD_2 target irradiated with $68\ \text{J}$ ($7 \times 10^{19}\ \text{W cm}^{-2}$) on target. Notice that there are no neutrons at $2.45\ \text{MeV}$ above the detection threshold of the instrument.

Figure 1 is the neutron spectrum obtained when a bare CD_2 target was irradiated with $286\ \text{J}$ on target. The signature at $2.45\ \text{MeV}$ is clearly visible and is much larger than the background level. The apparent asymmetry in the neutron spectrum at energies of $\sim 5\ \text{MeV}$ is likely due to the instrument response of the detector—it was not able to record neutrons below $1.8\ \text{MeV}$ due to the available time window. A Gaussian fit to the neutron spectrum at this energy revealed a full width at half maximum (FWHM) of $1.04\ \text{MeV}$ in this shot, corresponding to an ion temperature of $161\ \text{keV}$ [9]. Figure 3 shows the spectrum produced with a $10\ \mu\text{m}$ -thick CH_2 overlay thickness with $400\ \text{J}$ on target. The width is now significantly reduced and the FWHM of the Gaussian fit is $90\ \text{keV}$, corresponding to an ion temperature of $1.2\ \text{keV}$. The signals at $2.45\ \text{MeV}$ for thicker CH_2 overlays ($>10\ \mu\text{m}$) had much poorer statistics, particularly as these had the same signal height as background beam-fusion neutrons. Consequently, the deconvolution of the temperature from these more deeply buried layers is more uncertain, and they are therefore not discussed further in this letter.

Figure 5 shows the relative neutron yields plotted on the left-hand axis against deduced temperature and the fusion reaction rates on the right-hand axis. Within the standard deviation of the measurements, they are found to be consistent with that calculated using the standard thermonuclear fusion model with a fixed volume and confinement time. The absolute $2.45\ \text{MeV}$ neutron yield is in the range 2×10^6 – 4×10^7 and corresponds to a transfer of incident laser energy to the CD_2 plasma of $\sim 1\%$.

Figure 6 shows the inferred ion temperature as a function of the front CH_2 overlay thickness. Also plotted are electron temperatures calculated using Mission Research Corporation's LSP simulation tool reported in the literature that most clearly agree with the measured background electron temperatures obtained under similar irradiation conditions [3]. It can be seen from the plot that the ion temperature in the surface layers is very much larger than that expected from simulations.

The apparent absence of beam-fusion neutrons around $2.45\ \text{MeV}$ in these measurements is explained by the formation of a hole-boring channel along the laser axis [10]. The subsequent

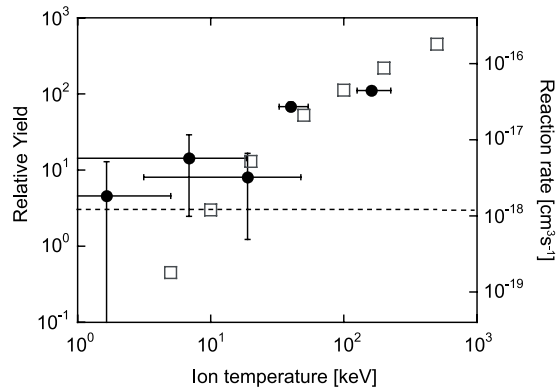


Figure 5. The relative neutron yields (●, related to the left-hand axis) against deduced temperature. The fusion reaction rates (□, related to the right-hand axis) for these temperatures are also plotted. The detection threshold is plotted as the horizontal dashed line.

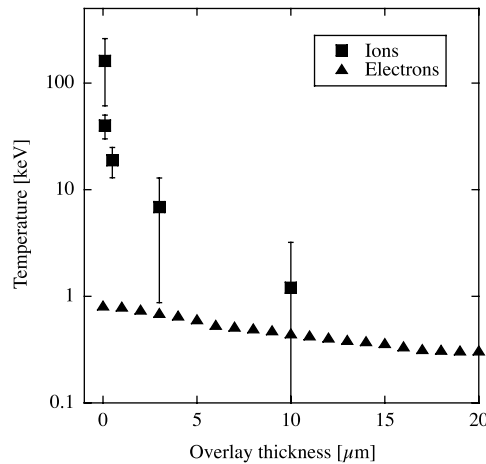


Figure 6. Ion temperature as a function of overlay thickness. Also plotted is the closest fit LSP simulation to electron temperature measurements made under similar irradiation conditions from [3]. The errors on each data point were estimated from fitting Gaussian profiles to the 2.45 MeV neutron spectra, as discussed in the caption to figure 1.

Coulomb explosion of the channel is in the radial direction, perpendicular to the laser beam direction. The angular distribution of the generated beam fusion neutrons is outside the observation solid angle of the LaNSA instrument. The higher energy beam-fusion neutrons seen in the data could be generated by filament coalescence [11, 12] or anomalous resistivity associated with fluctuating magnetic fields inducing chaotic orbits of the fast electrons [13]. Distinguishing these possibilities will be the subject of further experimental investigation.

We propose that the ion heating is caused by the ion instability described by Mendonça *et al* [14], driven by electron perturbations caused by the passage of the fast electrons accelerated into the target by the laser pulse. They showed that when the leading second order term is included in the plasma dispersion relation, derived from linearized, electrostatic fluid equations, the ion dispersion relation (low frequency root of the plasma dispersion relation) becomes coupled to the electron dispersion relation (high frequency root) by a term in the energy density of the

electron perturbations. They then showed that this leads to an ion instability when the group velocity of the electrons is comparable to the phase velocity of the ions, which is approximately the ion sound speed. In our case the group velocity will be given by the drift velocity, which will almost certainly exceed the ion sound speed, and the initial magnitude of the electron density perturbation will be given by the fast electron density n_f . Under these circumstances and neglecting collisions and any growth in the electron perturbations due to electron instabilities, it can be shown that the maximum growth rate of the ion instability is given by

$$\Gamma_{\max} = \left(\frac{m_e}{16m_i} \right)^{1/3} \left(\frac{n_f}{n_e} \right)^{2/3} \omega_{pe}, \quad (1)$$

where the subscripts e and i denote electron and ion quantities and other symbols have their usual meaning. To obtain a higher ion temperature than electron temperature the energy in the electron perturbations must be transferred to the ions faster than it is transferred to electron heating, which requires the growth rate to exceed the electron collision frequency. To give the growth rate in terms of the laser parameters we will use $n_f \approx f_{\text{ab}} I / \langle K_f \rangle c$ and assume that the mean fast electron energy $\langle K_f \rangle$ is given by the ponderomotive potential in the strongly relativistic limit. For the electron collision frequency we will use the rate of angular scattering from the atoms of an electron travelling at the drift velocity $v_d \approx (n_f/n_e)c$, assuming that the drift velocity exceeds the thermal velocity. This gives

$$I > 10^{20} \left(\frac{0.5}{f_{\text{abs}}} \right)^2 \left(\frac{\lambda}{\mu\text{m}} \right)^2 \left(\frac{n_e}{4 \times 10^{22} \text{ cm}^{-3}} \right)^{25/11} \left(\frac{Z_s \ln \Lambda}{4} \right)^{6/11} \text{ W cm}^{-2}, \quad (2)$$

where λ is the laser wavelength, $4 \times 10^{22} \text{ cm}^{-3}$ is the number density of CH_2 in polyethylene and $Z_s \ln \Lambda$ comes from the electron scattering term. This intensity threshold is consistent with that observed in the experiments, but an exact comparison cannot be made since it is strongly dependent on the absorption and electron density, which are not well known. It is likely, however, that this ion heating phenomenon will be restricted to low Z materials with the intensities that are available with present-day PW-class lasers.

The measurements suggest an alternative approach to hot spark formation in fast ignition where one relies on this instability to heat the core rather than collisions. Malkin and Fisch [15] suggested a similar approach to hot spark formation based on Langmuir turbulence. This might be achieved by using a higher intensity femtosecond rather than a picosecond laser pulse, provide that this is compatible with the growth rate of the coupled instability in the deuterium–tritium fuel and, in the case of cone-guided fast ignition geometries [16–19], in the guide cone, where the excitation of the instability should be avoided to minimize energy losses. Indeed, this instability is a plausible candidate to explain the high PW laser to thermal energy conversion efficiency observed in the recent experiments conducted at Osaka University [17, 18]. Equation (2) indicates that the intensity threshold for the instability growth is reduced in the lower density, outer regions of the compressed CD core that is formed at the end of the guide cone at the stagnation of the implosion, in agreement with the experimental conditions. These measurements indicate that Hain and Mulser's coronal ignition model could become a viable option for fast ignition [20].

Neutron time of flight signals were observed in the Vulcan petawatt laser facility at Rutherford Appleton Laboratory using the LaNSA system. The obtained spectra had two distinct features: a high-energy component that can be described in terms of beam-fusion reactions and a component around 2.45 MeV that can be described in terms of thermonuclear fusion. The ion temperatures calculated from the neutron signal width clearly demonstrate a dependence on the front CH_2 thickness of the layered target and are significantly higher than background electron temperatures measured under similar conditions. The ion heating process

is intensity dependent and is not observed with laser intensities on target below $10^{20} \text{ W cm}^{-2}$. The measurements are consistent with an instability that cascades the laser energy directly to the ions without significant background electron heating. They provide insight into the reduced electron heating observed by x-ray spectroscopy [3]. The implications for fast ignition are very promising indeed, since energy transfer to the ion population is the primary requirement for the hot spark formation.

The authors gratefully acknowledge the support of the staff of the Central Laser Facility in the execution of this work as well as significant assistance from Craig Sangster and his team in the redeployment of the LaNSA instrument. This was supported by the United Kingdom's Engineering and Physical Sciences Research Council and the Council for the Central Laboratory of the Research Councils. The Greek colleagues acknowledge support from the European Union. The Japanese colleagues acknowledge support from the Japan Society for the Promotion of Science.

References

- [1] Tabak M *et al* 1994 *Phys. Plasmas* **1** 1626
- [2] Koch J A *et al* 2001 *Phys. Rev. E* **65** 016410
- [3] Evans R G *et al* 2005 *Appl. Phys. Lett.* **86** 191505
- [4] Bell A R, Davies J R and Guerin S M 1998 *Phys. Rev. E* **58** 2471
- [5] Danson C N *et al* 2004 *Nucl. Fusion* **44** S239–S246
- [6] Cable M, Hatchett S P and Nelson M B 1992 *Rev. Sci. Instrum.* **63** 4823
- [7] Habara H, Lancaster K L and Norreys P A 2003 *CLF Annual Report 2002/2003 RAL Report* No RAL-TR-2003-018, pp 185–6, ISBN 0902376268
- [8] Norreys P A *et al* 1998 *Plasma Phys. Control. Fusion* **40** 175–82
Pretzler G *et al* 1998 *Phys. Rev. E* **58** 1165
Key M H *et al* 1998 *Phys. Plasmas* **5** 1966
Disdier L *et al* 1999 *Phys. Rev. Lett.* **82** 1454
Izumi N *et al* 2002 *Phys. Rev. E* **65** 036413
Habara H *et al* 2003 *Phys. Plasmas* **10** 3712
Habara H *et al* 2004 *Phys. Rev. E* **69** 036407
Habara H *et al* 2004 *Phys. Rev. E* **70** 046414
- [9] Slaughter D R 1989 *Rev. Sci. Instrum.* **60** 552
- [10] Pukhov A and Meyer-ter-Vehn J 1997 *Phys. Rev. Lett.* **79** 2686
- [11] Honda M, Meyer-ter-Vehn J and Pukhov A 2000 *Phys. Rev. Lett.* **85** 2128
- [12] Bret A, Firpo M C and Deutsch C 2005 *Phys. Rev. Lett.* **94** 115002
- [13] Sentoku Y, Mima K, Kaw P and Nishihara K 2003 *Phys. Rev. Lett.* **90** 155001
- [14] Mendonça J T and Bingham R 2002 *Phys. Plasmas* **9** 2604
Mendonça J T, Norreys P A, Bingham R and Davies J R 2005 *Phys. Rev. Lett.* **94** 245004
- [15] Malkin V M and Fisch N J 2002 *Phys. Rev. Lett.* **89** 125004
- [16] Norreys P A *et al* 2000 *Phys. Plasmas* **7** 3721
- [17] Kodama R *et al* 2001 *Nature* **412** 798
- [18] Kodama R *et al* 2002 *Nature* **418** 933
- [19] Norreys P A *et al* 2004 *Phys. Plasmas* **11** 2746
- [20] Hain S and Mulser P 2001 *Phys. Rev. Lett.* **86** 1015